Characterization of an Epstein-Barr Virus Receptor on Human Epithelial Cells

By Mark Birkenbach,*‡§ Xiao Tong,‡ Laura E. Bradbury,§‖ Thomas F. Tedder,§‖ and Elliott Kieff*‡

*From the Departments of *Medicine, Brigham and Women's Hospital, ‡Microbiology and Molecular Genetics, and §Pathology, Harvard Medical School; and the ‖Division of Tumor Immunology, Dana Farber Cancer Institute, Boston, Massachusetts 02115*

Summary

Epstein-Barr virus (EBV) adsorption to human B lymphocytes is mediated by the viral envelope glycoprotein, gp350/220, which binds to the cell surface protein, CD21, also known as the CR2 complement receptor. Human epithelial cells also express an EBV receptor. A candidate surface molecule of 195 kD has previously been identified on an epithelial cell line and explanted epithelial tissue by reactivity with the CD21 specific monoclonal antibody (mAb), HB-5a. In experiments to further characterize the epithelial cell EBV receptor, we have found that two human epithelial cell lines, RHEK-1 and HeLa, specifically bind intact EB virions. A 145-kD protein, similar in size to B lymphocyte CD21, was specifically precipitated from surface iodinated RHEK-1 cells using the HB-5a mAb, or using purified soluble gp350/220 coupled to agarose beads. The previously identified 195-kD protein did not bind to gp350/220 or react with two other anti-CD21 mAbs. CD21 homologous RNA, similar in size to the B lymphocyte CD21 mRNA, was detected in both RHEK-1 and HeLa cells. The nucleotide sequence of the epithelial cell cDNA was identical to B lymphocyte CD21. The longest clone differs from previously reported CD21 cDNAs in having additional 5′ untranslated sequence. Polymerase chain reaction amplification of RHEK-1- or B lymphoblastoid-derived cDNA verified that most CD21 transcripts are initiated at least 30–50 nucleotides upstream of the previously reported mRNA cap site. These experiments demonstrate that human epithelial cells can express CD21, and that CD21 is likely to mediate EBV adsorption to epithelial cells.

EBV is a human herpesvirus that causes infectious mononucleosis and has been associated with a variety of human lymphocytic and epithelial neoplasms, including Burkitt's lymphoma and nasopharyngeal carcinoma (for review see reference 1). Viral tropism for human B lymphocytes appears to be due in large part to restricted expression of the EBV receptor, CD21, which also serves as the lymphocyte receptor for the C3d,g component of complement, CR2 (2–5). EBV binding to CD21 is mediated by the viral envelope glycoprotein, gp350/220 (6), through a peptide that is highly homologous to a portion of the C3d,g ligand (7). After binding, virions are internalized through an endocytic mechanism that does not appear to involve clathrin-coated pits (8).

Nascent CD21 in B lymphocytes has an apparent molecular mass of 105 kD by SDS-PAGE (9), whereas the mature glycosylated form migrates at 145 kD (5, 9). Cloning and sequencing of CD21 cDNA and genomic DNA from B lymphocytes revealed an open reading frame that encodes a protein predicted to consist of a large extracellular amino-terminal domain comprising 15 or 16 structurally related short consensus repeats (SCRs)[1]; a hydrophobic transmembrane domain; and a short, intracellular COOH terminal tail (10–12). The CD21 transcript is highly spliced; each SCR domain or contiguous pair of SCRs is encoded by an individual exon or pair of exons (11). High resolution electron microscopy of negatively stained, purified CD21 polypeptide has demonstrated that the SCRs form an extended, linear structure (13). Recombinant molecular genetic epitope mapping has indicated that CD21 specific mAbs recognize determinants in separate SCR domains: HB-5a in SCR4 or 5; OKB-7 in SCR1; and B2 in SCR9 to 11 (14, 15). EBV gp350/220 binding is dependent upon partially defined structural features of SCRs 1 and 2, and is blocked by OKB-7 binding (14–16).

EBV infects epithelial cells as well as B lymphocytes. EBV genomes have been detected by in situ hybridization in desqua-

[1] *Abbreviations used in this paper:* RACE, rapid amplification of cDNA ends; SCR, short consensus repeat.

mated oropharyngeal epithelial cells of acute infectious mononucleosis patients (17), and in salivary gland epithelium of normal, seropositive adults (18). EBV DNA, RNA, and proteins are invariably present in the malignant epithelial cells of the nonkeratinizing variants of nasopharyngeal carcinoma (19). More recently, active replication of EBV genomes has been demonstrated in epithelial cells of AIDS-associated oral hairy leukoplakia (20, 21).

Attempts to characterize the epithelial cell membrane protein responsible for EBV adsorption have yielded inconsistent results. Epithelial cells express an antigen recognized by some CD21 specific mAbs, in particular HB-5a (18, 22–26). A recent report described the identification of a 195–200-kD protein in epithelial cells which could be specifically precipitated by HB-5a (22). However, other CD21-specific mAbs did not react with this protein. The objective of this study was to identify and characterize the EBV receptor on epithelial cells. These experiments were undertaken using two epithelial cell lines, HeLa and RHEK-1 (27). The latter had previously been shown to exhibit HB-5a mAb reactivity (28).

Materials and Methods

Cell Lines. RHEK-1 (generous gift from Dr. Jong Rhim, National Cancer Institute, Bethesda, MD) is a human keratinocyte line that was generated by infection of primary foreskin epithelial cells with an adenovirus 12/SV40 hybrid virus (27). These cells display ultrastructural features of well-differentiated keratinocytes forming cytokeratin tonofilaments and desmosomes. Though immortalized, RHEK-1 cells are not fully malignant and fail to form colonies in soft agar or tumors in nude mice. HeLa is a human epithelial line established from a primary cervical adenocarcinoma (29) and has also been previously shown to express cytokeratins (30). Molt-4 is a human T lymphocyte line that was previously reported to express a CR2 related antigen (2, 5). IB4 is an EBV-immortalized B lymphoblastoid cell line. Raji is an EBV-infected Burkitt tumor cell line that expresses relatively large amounts of CD21 (6). K562 is a Philadelphia chromosome-positive human chronic myeloid leukemia cell line (6a) that does not express CD21 (5).

Antibodies. The mAbs used in this study include: HB-5a (CD21, IgG2a [5]), HB-5b (CD21, IgG1), HB-5c (CD21, IgG1), B2 (CD21, IgM [31], obtained from Coulter Immunology, Hialeah, FL); OKB-7 (CD21, IgG2b [3], obtained from Ortho Diagnostics, Raritan, NJ); HB-12b (CD19, IgG1 [2]), 5A6 (anti-TAPA-1, IgG1, a generous gift from Dr. Shoshana Levy, Stanford University, Palo Alto, CA [33]); and anti-Leu-13 (IgG1, a generous gift from Dr. Robert Evans, Roswell Park Memorial Institute, Buffalo, NY [34]). The HB-5b and HB-5c antibody producing hybridomas were generated by the fusion of NS-1 myeloma cells with spleens of mice immunized with the BJAB cell line. The HB-5b and HB-5c antibodies generated reactivity patterns with hematopoietic cells similar to those of the HB-5a antibody, immunoprecipitated a 145,000 M_r B lymphocyte surface molecule, and reacted with CD21 cDNA-transfected K562 cells, but not parental cells. The CD21 epitopes identified by the HB-5b and HB-5c antibodies were different from the epitope identified by the HB-5a antibody since the prior binding of those antibodies did not block HB-5a antibody binding.

Indirect immunofluorescence analysis was carried out after washing the cells twice. Suspensions of viable cells were analyzed for surface Ag expression by incubation for 20 min on ice with the appropriate mAb as ascites fluid diluted to the optimal concentration for immunostaining. After washing, the cells were treated for 15 min at 4°C with FITC-conjugated goat anti-mouse Ig antibodies (Southern Biotechnology Associates, Birmingham, AL). Single-color immunofluorescence analysis was performed on a flow cytometer (Epics Profile; Coulter Electronics, Hialeah, FL). 10^4 cells were analyzed in each instance and all histograms are shown on a three decade log scale. For immunofluorescent visualization of membrane CR2, live cells were incubated in chamber slides with the CR2-specific mAbs HB-5a, OKB-7, and B2.

Virus Binding. RHEK-1 and HeLa cells were grown overnight in 8-well chamber slides (Nunc, Inc., Naperville, IL) at an initial density of 10^5 cells/ml. Raji cells were grown in suspension to a density of 10^6 cells/ml. Cells were washed with PBS plus 10% goat serum, and incubated with B95–8 virus (virus titer: 10^8 transforming units/ml) for 1 h on ice. After washing with PBS, cells were incubated for 1 h on ice with 2L10 mAb, specific for the EBV envelope glycoprotein gp350/220 (gift of Dr. G. Pearson, Georgetown University, Wash. DC). FITC-conjugated goat anti-mouse antibody was added. Cells were visualized under epifluorescence with a Zeiss Axiomat photomicroscope (Thornwood, NY).

RNA Analysis. Total cellular RNA was purified by acid guanidinium phenol chloroform extraction (35). The polyadenylylated RNA fraction was isolated by oligodeoxythymidine cellulose chromatography. RNA samples (IB4, 4 μg/lane; all other samples, 10 μg/lane) were size fractionated in 0.66 M formaldehyde, 0.8% agarose, blotted onto activated nylon membrane, and hybridized with a ^{32}P-labeled, CD21 specific probe. The probe was generated using a previously described cDNA clone isolated from the B lymphocyte cell line Raji (36) and consists of the 1.76- and 1.45-kb EcoRI fragments that comprise the open reading frame. After washing under conditions of moderate stringency (25°C below melting temperature), the filter was exposed to preflashed film (Kodak XAR; Eastman Kodak Co., Rochester, NY) for 7 d. Relative RNA abundance levels were determined by direct densitometric scanning of autoradiographs using a spectrophotometer (model DU-8; Beckman Instruments, Inc., Fullerton, CA) equipped with a slab gel Compuset module (Beckman Instruments, Inc.), and corrected for the total amounts of RNA loaded in each lane.

cDNA Library Preparation. 5 μg of polyadenylylated RHEK-1 RNA was reverse transcribed using Moloney murine leukemia virus reverse transcriptase (Super Script; Bethesda Research Laboratories, Gaithersburg, MD). Second-strand synthesis was performed using *Escherichia coli* DNA polymerase I and ribonuclease H. After methylation, linker ligation, and EcoRI restriction digestion, the cDNA was size selected by Sepharose 4B gel filtration chromatography, and cloned into λgt10. $\sim 2 \times 10^6$ recombinant phage were screened by in situ plaque hybridization using ^{32}P-labeled CD21 specific probe. Positive clones were plaque purified and cDNA inserts were subcloned into pBluescript (Stratagene Inc., La Jolla, CA) for sequence analysis.

PCR Amplification. The "rapid amplification of cDNA ends" (RACE) procedure of Frohman et al. (37) was used to characterize the 5′ ends of CD21 transcripts. First-strand cDNA synthesis was performed on 2.5 μg of polyadenylylated RNA from RHEK-1 or IB4 cells, using the oligonucleotide primer, CR2–8 (ATGTCCATTGTGGATCATA) complementary to a region in the third exon of the CR2 mRNA. The cDNA products were polydeoxyadenylate tailed using terminal deoxynucleotidyl transferase and dATP. Products of a mock reverse transcription reaction, in which H_2O was added in place of RNA, were used in negative control amplifications. Initial amplification was carried out using the following oligonucleotide primers at the concentrations indicated: 0.2 μM

T adaptor (GCCTCGAGCTCTAGAATTCCTTCT$_{17}$); 1.0 μM adaptor (GCCTCGAGCTCTAGAATTCCT); and 1.0 μM CR2–10 (ACACAGGTTGGTAGTCGT). The CR2–10 primer matches a sequence in the second exon of the CR2 transcript. The amplification reactions were performed sequentially as follows: 94° 1 min, 48° 3 min, 72° 5 min (2 cycles); 94° 1 min, 50° 3 min, 72° 5 min (2 cycles); 94° 40 s, 53° 1 min, and 72° 3 min (35 cycles). 5 μl of the products of the first amplification were subjected to a second round of amplification using 1.0 μM Ad and 1.0 μM CR2–14 (ATTGAAGAATTCACATTTAGGAGCAGGTTTA) oligonucleotide primers. The CR2–14 primer is specific for a sequence in the second exon of the CR2 mRNA, upstream of primer CR2–10. Two nucleotide mismatches were incorporated in CR2–14 to generate an EcoRI restriction site to facilitate subcloning and analysis of amplification products. Amplification reaction conditions were 94° 1 min, 55° 2 min, and 72° 3 min (40 cycles). 15 μl of the second amplification reaction products were size fractionated in 1.2% agarose and transferred to charged nylon membrane (GeneScreen Plus; New England Nuclear, Billerica, MA). The filter was hybridized sequentially with the following ^{32}P-end-labeled oligonucleotide probes (see Fig. 3): CR2–11 (GCCCGCCTCTCCTGGCTCAC); CR2–12 (CTAGCACGTGTGCCGGACAC); and CR2–15 (TGCTTGCTGCTCCAGCCTTGC). CR2–11 and -12 correspond to sequences upstream of the transcriptional initiation site previously identified in Raji cells (12, 38). CR2–15 matches the sequence at the 5′ end of the Raji CR2 transcript (38). Filters were washed at 60°C in 0.5× SSC (20×SSC: 3.0 M NaCl, 0.3 M NaCitrate), 1% SDS, and exposed 4–12 h to Kodak XAR film. The remainder of the IB4 cDNA amplification products were EcoRI digested, subcloned into pBluescript, and sequenced.

Protein Labeling. Confluent cultures of 2–3 × 10^8 RHEK-1 epithelial cells were removed from plates by scraping in ice-cold PBS/1 mM EDTA, pelleted, and washed once with PBS. Suspension cultures of Raji cells (10^7) were pelleted directly and washed once in PBS. After resuspending in PBS, cells were incubated 15 min at 4°C with the water-soluble Bolton-Hunter reagent, sulfosuccinimidyl-3-(4-hydroxyphenyl)propionate (sulfo-SHPP, Pierce Chemical Co., Rockford, IL) at 0.2 mg/ml. Cells were washed twice, suspended in PBS, and radioactively labeled using lactoperoxidase and ^{125}I (1.0 mCi/ml). For metabolic labeling studies, RHEK-1, HeLa, and IB4 cells were grown to 10^6 cell/ml. Labeling was carried out overnight by addition of 1 mCi [^{35}S]methionine (New England Nuclear) to 10^8 cells in methionine-free DMEM medium supplemented with 10% dialyzed fetal bovine serum.

Purification of Soluble gp350/220. Gp350/220 was purified by the previously described ion-exchange chromatography procedure (39) from the supernatants of GH3-Δ19 cells grown in DMEM supplemented with 5% FCS. These cells constitutively secrete a soluble form of gp350/220 lacking the transmembrane domain of the viral envelope protein (40). Cell supernatants were adjusted to 20 mM piperazine, pH 5.4, 0.5% NP-40, 0.1 M betaine (buffer A). The supernatant was run through a MonoQ XK 16/20 preparative column (Pharmacia/LKB, Piscataway, NJ), at a flow rate of 2 ml/min. The column was washed with buffer A at a flow rate of 1.25 of ml/min, and eluted by 150 ml 0–0.5 M NaCl linear gradient. Fractions were assayed by Western blot using 2L10 primary antibody. Samples containing gp350/220 were pooled, diluted 1.5-fold in buffer A, and applied to a second MonoQ HR 5/5 analytical column at a flow rate of 1.0 ml/min. The column was washed with buffer A and eluted with 30 ml 0–0.5 M NaCl linear gradient. Fractions containing gp350/220 were collected and incubated with Jacalin-agarose (Sigma Chemical Co., St. Louis, MO) for 4 h at 4°C. The agarose beads were washed with PBS, then eluted with 0.1 M methyl-a-galactopyranoside in PBS. The eluate was dialyzed against PBS and concentrated by centrifugation on Centricon-100 filters (Amicon Corp., Beverly, MA). Total protein yield was determined by the Bradford Coomassie stain assay (Bio-Rad Laboratories, Richmond, CA). ~8 μg of the final purification product was analyzed by SDS-PAGE. Proteins were visualized by silver staining (Bio-Rad Laboratories).

Coupling of Reagents to Affi-Gel. Antibody HB-5c (0.5 mg/ml) was coupled to agarose beads (Affi-Gel 10, Bio-Rad Laboratories); BSA (0.5 mg/ml) and gp350/220 (0.3 mg/ml) were coupled to Affi-Gel 15 agarose beads. The coupling was done by incubating the protein solution with beads for 4 h at 4°C. The unreacted coupling sites were blocked by 0.2 M glycine. The coupled agarose beads were washed with PBS and stored at 4°C.

Immunoprecipitation of CR2. Labeled cells were lysed in buffer (10^8 cell/2 ml lysis buffer) containing 120 mM NaCl, 10 mM Tris (pH 7.5), 1% NP-40, 2 μg/ml aprotinin, 1 mM PMSF. Insoluble material was removed by centrifugation. The lysates were precleared with agarose beads coupled with BSA for 2 h at 4°C, and were divided into replicate samples. Agarose beads coupled with the CR2-specific mAbs HB-5a (5), HB-5b, HB-5c, purified soluble gp350/220, or BSA were added to each sample, respectively. The lysates were incubated with beads overnight. The immunoprecipitated samples were run on 7.0% SDS-PAGE and visualized by autoradiography.

Results

As expected from previous studies of human epithelial tissues and cell lines, the HB-5a antibody recognized an antigen on the plasma membranes of live RHEK-1 and HeLa cells in indirect immunofluorescence assays (data not shown). In contrast, two other CD21 specific mAbs, OKB-7 and B2, yielded only weak or equivocal membrane fluorescence (data not shown), which is consistent with previous studies of epithelial cells. All three antibodies reacted with the plasma membranes of live Raji cells, an EBV-positive Burkitt lymphoma cell line, though reactivity with OKB-7 was consistently weaker than with B2 or HB-5a (data not shown). These results confirm the previous inconsistency in the reactivity of CD21-specific mAbs with an epithelial cell surface antigen (18, 22–26).

Virus Binding. RHEK-1 and HeLa epithelial cells bound intact EB virions, albeit to a lesser extent than B lymphocytes. Concentrated preparations of B95–8 virus were incubated with subconfluent RHEK-1 or HeLa cells cultured in chamber slides. After extensive washing, immunofluorescence staining was performed using the mAb 2L10, specific for EBV envelope glycoprotein, gp350/220. Although this glycoprotein has previously been shown to mediate EBV binding to CR2, the epitope recognized by 2L10 is distinct from the CR2 binding domain (6, 7). Focal, punctate fluorescence representing viral particles was observed along cytoplasmic membrane margins in both RHEK-1 and HeLa cells (Fig. 1 *c*, *e*, and *g*). The majority of RHEK-1 cells bound variable numbers of virions, ranging from one to several virions per cell. The selected fields depicted show somewhat higher levels than were generally observed. RHEK-1 cell virus binding levels were typically 5- to 10-fold lower than in IB4, a B lymphoblastoid cell line established by EBV infection of primary

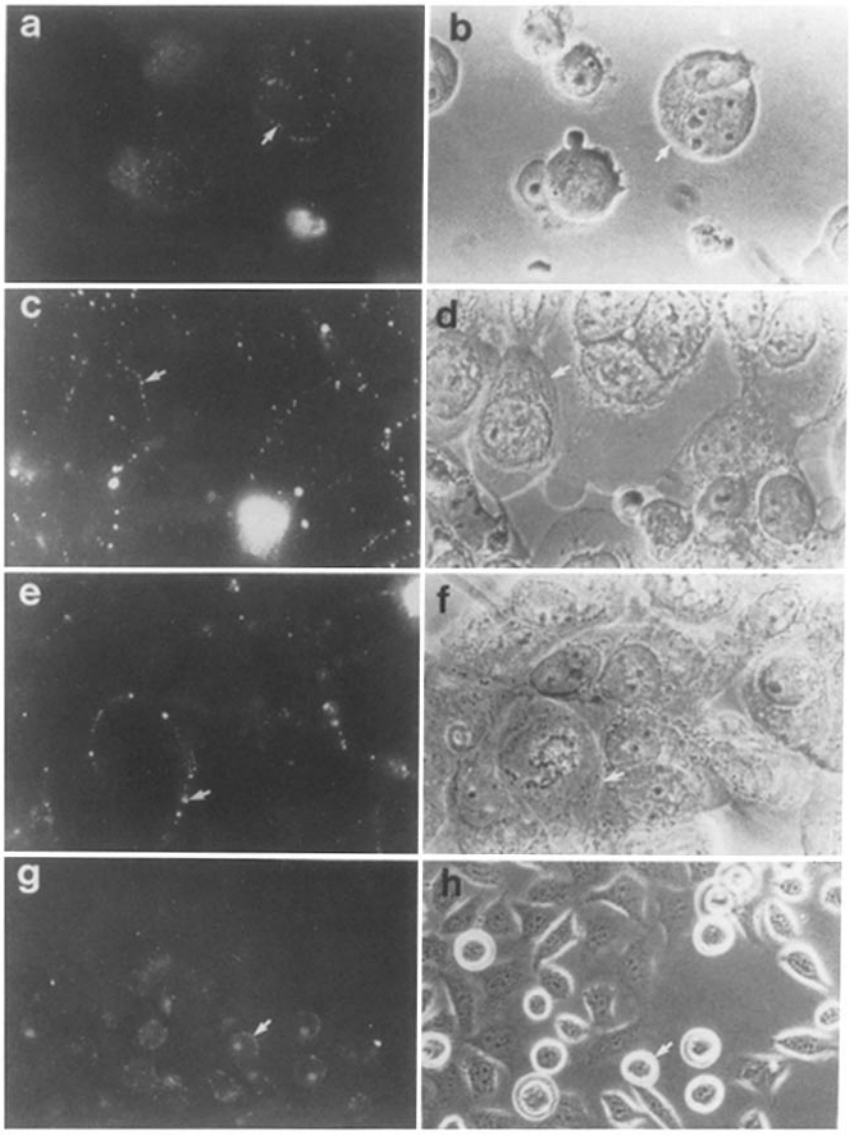

Figure 1. Immunofluorescence detection of Epstein-Barr virion binding to epithelial cells. Concentrated EB virus stocks (10^8 transforming U/ml) were incubated for 1 h with epithelial cell cultures in chamber slides. Cells were washed and stained with the mAb, 2L10, specific for the viral envelope glycoprotein, gp350/220. As a positive control, IB4 lymphocytes in suspension culture were similarly stained in microtiter wells and visualized. Bound EB virions are visualized as punctate fluorescent structures on the cell surfaces (*white arrows*; *a*, *c*, *e*, and *g*). Corresponding cell surfaces are indicated by white arrows in phase contrast images (*b*, *d*, *f*, and *h*) at the right of each immunofluorescence photomicrograph. Numerous virions are bound diffusely to the surfaces of IB4 B lymphoblastoid cells (*a*). Significantly fewer bound virions are observed along the cytoplasmic margins of RHEK-1 (*c* and *e*) and HeLa epithelial cells (*g*). *a–f*, ×1000; *g* and *h*, ×450.

B lymphocytes in vitro (Fig. 1 *a*). The substantially greater binding to nonadherent IB4 cells is not reflected in photomicrographs because these were restricted to a single focal plane (Fig. 1 *a*). HeLa cells on average bound significantly less virus than RHEK-1. In HeLa cultures, virus bound predominantly to the surfaces of rounded cells, in contrast to the more common flattened or spindle-shaped cells which did not bind virus detectably (Fig. 1, *g* and *h*). K562, a chronic myeloid leukemia-derived cell line that does not express CD21 was used as a negative control for virus binding. No fluorescence was observed with the negative control line K562 after incubation with virus and 2L10 antibody, or with epithelial cells that had not been incubated with virus (data not shown).

RNA Analysis. The RHEK-1 and HeLa cell reactivity with HB-5a mAb and virus binding properties are compatible with the hypothesis that the EBV receptor protein is encoded by a CD21-homologous mRNA. The absence of significant reactivity with B2 and OKB-7 would necessitate a more complicated model such as preservation of some but not all CD21 epitopes because of differential splicing. To pursue this hypothesis, RNA was extracted, size fractionated on a formaldehyde agarose gel, and hybridized with a CD21-specific probe at moderate stringency. A 4.3-kb RNA was detected in RHEK-1 cell RNA (Fig. 2), matching in size the more abundant, predominant CD21 RNAs of the B lymphocyte line, IB4 and the T cell line, Molt-4. An RNA species of identical size was detected at low levels in RNA extracted from HeLa cells. A number of less abundant CD21 homologous RNAs, both larger and smaller than the predominant 4.3-kb message, are evident in IB4, as have been observed in other B lymphocyte RNA preparations (11). None of these latter RNAs were detected in epithelial cell RNA preparations. A 0.55-kb RNA, however, was evident in HeLa and MOLT-4 RNA. In IB4 cells, the 4.3-kb RNA is ~50-fold more abundant than in RHEK-1 cells, and 90-fold more abundant than in HeLa cells as assessed by densitometric scanning

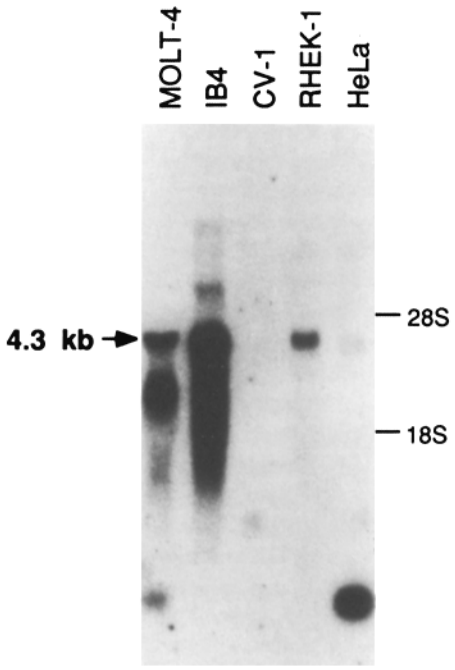

Figure 2. CR2 RNA expression in epithelial cell lines. RNA was isolated from the following cell lines: MOLT-4 (human T acute lymphoblastic leukemia cell line); IB4 (human B lymphoblastoid cell line); CV-1 (simian fibroblast); RHEK-1, and HeLa (human epithelial cell lines). 4 (IB4), or 10 μg (all other cell lines) polyadenylylated RNA was size fractionated, blotted, and hybridized to a ^{32}P-labeled CR2 probe. A 4.3-kb band, indicated by the arrow, is detected in MOLT-4, IB4, RHEK-1, and HeLa cells. Positions of ribosomal RNA bands are indicated by dashes (*18S*, *28S*). A 0.55-kb RNA species of unknown structure is detected in MOLT-4 and HeLa RNA.

of autoradiographs, normalized for total RNA loaded per lane. Thus the abundance of the CD21 homologous RNA in the epithelial cells correlates qualitatively with relative virus binding activity: IB4 > RHEK-1 > Hela.

To identify CD21 homologous RNA in human epithelial tissues, RNA was extracted from uterine cervical epithelium dissected from freshly excised surgical specimens and analyzed by RNA blot hybridization. A 4.3-kb RNA was specifically detected in this preparation with CD21 probe (data not shown). However, rehybridization of this blot with Igκ L chain probe readily detected significant quantities of κ mRNA. Thus, the epithelial tissue preparation was likely contaminated with lymphocytes or plasma cells.

The RHEK-1 RNA homologous to CD21 was cloned and sequenced to determine its precise relationship to the B lymphocyte message. A RHEK-1 RNA cDNA library was constructed and screened using a CD21 probe. Four independent cDNA clones were isolated from an initial screening of 2×10^6 recombinant bacteriophage. The structure of each clone was determined by restriction mapping and sequence analysis (Fig. 3 *A*). All four clones lacked the variable exon of the B lymphocyte CD21 mRNA (41), encoding the SCR domain designated either 10b (11) or 11 (13). Complete sequencing of the largest clone, RH50, indicated precise nucleotide identity with a previously published CD21 cDNA (11–13), though the untranslated leader sequence of the epithelial cDNA was longer than had been previously described for B lymphocyte CD21 (12, 38). The longer leader placed the transcriptional initiation site at least 11 (38) or 32 (12) nucleotides upstream of previously mapped B lymphocyte CD21 mRNA cap sites (Fig. 3 *B*).

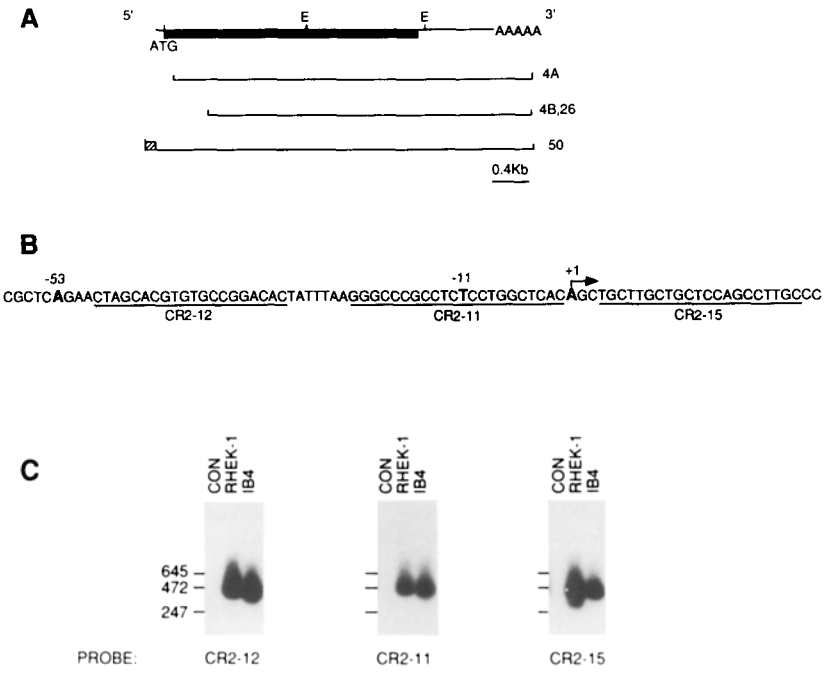

Figure 3. Structure of epithelial cell CR2 mRNA and cDNA clones. (*A*) Structure of the CR2 message is shown schematically at the top, indicating positions of the initiation codon (*ATG*), two EcoRI restriction sites (*E*), and polyadenylate tail (*AAAAA*). (*Filled box*) CR2 open reading frame. Structures of four independent CR2 cDNA clones (*4A*, *4B*, *26*, and *50*) from the epithelial cell line RHEK-1 are shown below. (*Hatched box* at the 5′ end of clone 50) Additional untranslated sequence upstream of the transcriptional initiation site previously identified in Raji B lymphocytes (32). (*B*) The highlighted nucleotide at position +1 (*rightward arrow*) represents the previously mapped Raji initiation site (32). The first nucleotides of RHEK-1 cDNA clone 50, and of the longest clone obtained by PCR amplification of IB4 cDNA, are highlighted at positions −11 and −53, respectively. (*Underlined bases*) Sequences of oligonucleotide probes CR2–11, CR2–12, and CR2–15. (*C*) Products of PCR amplification of polydeoxyadenylate tailed cDNA from IB4 and RHEK-1 cells were hybridized with ^{32}P-labeled oligonucleotide probes CR2–11, -12, and -15. The positions of DNA markers are shown (*left*) with sizes in base pairs indicated. All three probes detect prominent bands at ~430 nucleotides in both RHEK-1 and IB4 amplification products. Shorter exposure indicates the presence of a discrete minor band at ~380 nucleotides in RHEK-1 amplification products hybridized with the CR2–15 probe. No bands are detectable in control reaction products (*CON*).

The use of this novel CD21 transcriptional initiation site was further analyzed using the RACE technique (37) to amplify the 5′ ends of the IB4 B lymphocyte and RHEK-1 epithelial RNAs. RHEK-1 and IB4 first-strand cDNA preparations were made using an oligonucleotide primer complementary to a sequence encoding the third SCR. The cDNA was polydeoxyadenylate tailed and amplified sequentially using a 5′ poly-dA specific adapter primer, and nested 3′ primers specific for sequences in the second exon of the CR2 mRNA. This technique should amplify the beginning of all CR2 transcripts. A control amplification was performed in parallel on the products of a mock reverse transcription reaction to which H_2O was added in place of RNA. The products of the second amplification were blotted and hybridized with ^{32}P-end-labeled oligonucleotide probes from the 5′ untranslated sequence (CR2–15) and putative promoter region (CR2–11, 12) of the CR2 transcript (Fig. 3 *C*). Amplification primers were selected to span one splice junction. As the size of the intervening intron exceeds 10 kb (11, 38), detection of amplified genomic DNA or unprocessed primary transcript is not possible. Specific products were routinely detectable after initial amplification of IB4 B lymphocyte cDNA. Specific products from RHEK-1 cDNA, however, were not detectable at this stage, necessitating the second amplification step. All three probes detected diffuse bands of similar size (~430 bp) in both IB4 and RHEK-1 amplification products. Short exposure autoradiographs indicate that the apparent slight discrepancy in size between IB4 and RHEK-1 products detected with the CR2–12 probe is due to trailing off of higher and lower molecular weight products above and below predominant bands of identical size in each lane. This artefact was not observed in multiple other hybridizations (data not shown). Given the size of the poly-dA adapter primer (40 nucleotides), these products map the transcriptional initiation site at or near 50 nucleotides upstream of the previously published mRNA cap site. Smaller products corresponding to transcripts initiated at either of the previously identified Raji cap sites (12, 38) were not evident in amplification products from IB4 B lymphocyte RNA. A minor band of ~380 bp was, however, detected after prolonged exposure of CR2–15 probe hybridized RHEK-1 amplification products (Fig. 3 *C*). Sequencing of three pBluescript clones of IB4 PCR products indicated heterogeneity in the start sites within a 25-bp region, the longest clone initiating at position −53 (Fig. 3 *B*). Amplification of HeLa cDNA with the CR2–12 and -14 oligonucleotide primers confirmed transcriptional initiation from this region in these cells as well (data not shown).

CD21 Immunoprecipitation. The preferential reactivity of epithelial cells with the HB-5a mAb versus B2 and OKB-7 in the face of an identity to B lymphocyte CD21 at the RNA level could be due to crossreactivity of HB-5a with another epithelial cell surface protein, to a difference in posttranslational processing of CD21 in epithelial cells or to partial occlusion of the B-2 and OKB-7 epitopes because of another epithelial cell surface protein. A 195-kD epithelial cell surface protein had previously been described to react with HB-5a. To investigate further the basis for the HB-5a reactivity and the relationship of the 195-kD protein to CD21, immunoprecipitations were performed using HB-5a and two other CD21-specific mAbs, HB-5b and HB-5c. As expected, all three reagents precipitated a 145-kD protein from [^{35}S]methionine-labeled extracts of the B lymphocyte line, IB4 (Fig. 4 *A*). The HB-5c-coupled beads were somewhat variable in their reactivity and slightly less efficient than HB-5a, whereas the HB-5b reagent was considerably less active (Fig. 4 *A*). A single 195-kD protein was clearly identified in HB-5a immunoprecipitations from both RHEK-1 and HeLa cells (Fig. 4, *A* and *B*). The HB-5b and HB-5c antibodies, however, consistently failed to precipitate this protein from RHEK-1 cells. Since HB-5c reactivity with IB4 CD21 was almost as strong as HB-5a, the failure to precipitate the 195-kD protein with HB-5c is confirmative of the previous observation that the 195-kD protein lacks other CD21 epitopes.

To increase the sensitivity of these assays RHEK-1 cells were surface labeled with ^{125}I, lysed in nonionic detergent, and the HB-5a reactive proteins were identified. Proteins of 195 and 145 kD were specifically precipitated from RHEK-1 cell lysates by the HB-5a mAb (Fig. 5 *A*). The less prominent 145-kD protein was identical in size to CD21 precipitated with HB-5a from surface-labeled Raji cells and run as a control in parallel (data not shown).

To ascertain which of these proteins is a receptor for the EBV gp350/220 ligand, ^{125}I surface-labeled RHEK-1 cell lysates were reacted with gp350/220 bound to an inert matrix. Recombinant gp350/220 consisting of the entire external domain is an efficient CD21 ligand (40). This reagent specifically precipitated a 145-kD protein from ^{125}I labeled RHEK-1 cells, and a protein of identical size from Raji B lymphocytes processed in parallel (Fig. 5 *B*). It is significant that in this and multiple other experiments, the 195-kD protein was not precipitated by gp350/220 (Fig. 5 *B*). However, the 195-kD protein was readily recovered from the supernatants of the gp350/220 precipitation after specific removal of gp350/220 bound material (Fig. 5 *C*, lane HB5a). In contrast, HB-5a precipitation of this supernatant no longer detected the 145-kD protein, indicating that it had been quan-

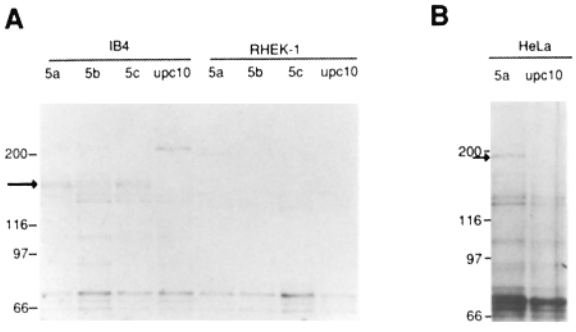

Figure 4. Immunoprecipitation of the 195-kD protein. IB4, RHEK-1 (*A*), and HeLa cells (*B*) were metabolically labeled with [^{35}S]methionine overnight. Lysates from 10^7 cells were precipitated with three CR2-specific mAbs, HB-5a (*5a*), HB-5b (*5b*), HB-5c (*5c*), and the control antibody Upc10 (*upc10*). All three CR2 antibodies precipitate the 145-kD CR2 protein from IB4 B lymphocytes (*A*, *large arrow*). A 195-kD protein (*small arrow*) is precipitated only by HB-5a from both RHEK-1 (*A*) and HeLa cell lysates (*B*).

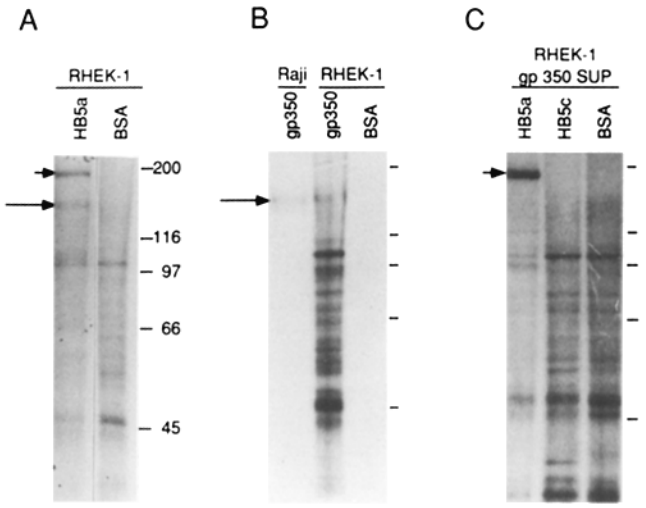

Figure 5. Immunoprecipitation of epithelial CR2. Raji and RHEK-1 cells were ^{125}I-surface labeled. Direct precipitation of RHEK-1 lysates with HB-5a specifically detects both the 195-kD (*small arrow*) and 145-kD (*large arrow*) proteins (*A*). Cell lysates from 2 × 10^6 Raji cells or 9 × 10^7 RHEK-1 cells were precipitated with purified soluble gp350/220 (gp350) or BSA coupled to agarose beads (*B*). A band at 145 kD (*large arrow*) is evident in both Raji and RHEK-1 gp350/220 precipitates, but is absent from BSA precipitates of RHEK-1 lysates. The 195-kD protein precipitable with HB-5a is not detected in the gp350/220 precipitation. (A diagonal split in the gel arose during drying but is located above the expected position of the 195-kD protein and did not involve any loss of gel material.) The RHEK-1 cell supernatant after gp350/220 precipitation (RHEK-1 gp350 Sup) was reprecipitated with two CR2-specific mAbs, HB-5a (*HB5a*) and HB-5c (*HB5c*), and with BSA control beads (*C*). The 145-kD CR2 protein is not detectable in this supernatant. A 195-kD protein (*small arrow*) is specifically precipitated from the supernatant by HB-5a but not by HB-5c.

titatively removed from the epithelial cell lysate by the gp350/220 coupled beads (Fig. 5 *C*, lane HB5a). These experiments demonstrate that RHEK-1 cells have on their surface a small amount of a 145-kD protein indistinguishable from CD21, and that the 195-kD protein does not interact with gp350/220.

Immunoprecipitation of ^{35}S-or ^{125}I-labeled HeLa extracts with HB-5a antibody consistently detected the 195-kD protein but failed to identify the 145-kD species (Fig. 4 *B* and data not shown). This finding was not unexpected given the small amount of the 145-kD protein detected in RHEK-1 cells, and the significantly lower abundance of the CD21 RNA in these cells as compared with RHEK-1.

Expression of CD19, TAPA-1, and Leu-13 by Cell Lines. The CD21 protein forms a complex with multiple cell surface molecules on lymphocytes (42) including CD19 (43), TAPA-1 (33), and the Leu-13 antigen (44). Since this multimolecular complex may be significant in CD21 function, the distribution of each protein on cell lines used in this study was examined by flow cytometry after reaction with specific antibodies (Fig. 6). As has been previously found on B lymphoblastoid cell lines, no strict correlation between the patterns of expression of these four antigens was found. CD21, CD19, TAPA-1, and Leu-13 were expressed by the IB4 B cell line, TAPA-1 and Leu-13 were expressed by RHEK cells, and TAPA-1 was expressed by HeLa cells. These results are consistent with

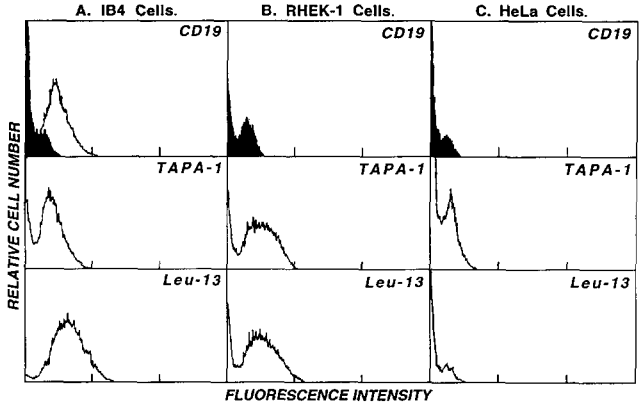

Figure 6. Expression of CD19, TAPA-1, and Leu-13 by epithelial cell lines. Cell surface antigen expression was determined by indirect immunofluorescence staining with flow cytometry analysis. Background staining obtained with unreactive mouse Ig as a control is shown as a filled histogram (*top*). Staining results obtained with the indicated antibodies, CD19 (HB13b), TAPA-1 (5A6), and Leu-13 are shown as open histograms. Fluorescence intensity is shown on a three decade log scale.

the prior observation that CD19 and CD21 can independently associate with TAPA-1, which independently associates with the Leu-13 protein (42).

Discussion

These experiments demonstrate that the human keratinocyte cell line, RHEK-1, expresses low levels of CD21 RNA; that the low RNA level correlates with a low level of expression of a protein similar in size and HB-5a reactivity to B lymphocyte CD21; that the 145-kD protein binds to the EBV ligand, gp350/220; and, that the low level CD21 expression correlates with a low level of EBV receptor activity. Thus, CD21 is almost certain to be the EBV receptor on RHEK-1 cells. A previously described 195-kD protein (22) was precipitable with HB-5a, but failed to bind gp350/220 or to react with the other anti-CD21 antibodies, HB-5b and HB-5c.

The similar size of the CD21 glycoprotein in epithelial cells and B lymphocytes is expected given the RNA sequence identity and the consistent size of CD21 glycoprotein previously noted in a variety of cell types, including murine L cell fibroblasts (45), Rat-1 fibroblasts (X. Tong, unpublished observations), SVK and SCC human keratinocytes (36), and the human myeloid leukemia cell line K562 (F. Wang, unpublished observations) after transfection with B lymphocyte CD21 cDNA under control of a heterologous promoter. These results suggest similar patterns of posttranslational processing of CD21 polypeptide in diverse tissues. Moreover, expression of the B lymphocyte CD21 cDNA in SVK or SCC keratinocytes renders these cells susceptible to EBV infection in vitro (36), confirming that this glycoprotein can serve as a functional viral receptor in epithelial cells.

It is likely that the CD21 expression in the RHEK-1 cell line represents a normal feature of epithelial cells rather than a consequence of idiosyncratic or global transcriptional activation in a transformed cell line. First, RHEK-1 cells exhibit a remarkably well-differentiated phenotype in vitro, synthesizing the epithelial marker protein, keratin, and forming

ultrastructural elements characteristic of keratinocytes, including tonofilaments and desmosomes (27). These cells are not fully transformed as evidenced by their failure to form tumors in nude mice or colonies in soft agar. Second, the CD21 RNA is expressed in an independent epithelial cell line, HeLa, which also synthesizes cytokeratins, but displays phenotypic features and growth characteristics distinct from those of RHEK-1. Third, RHEK-1 cells do not inappropriately express other markers of B lymphocyte differentiation, such as κ L chain transcripts (data not shown). Together these findings suggest that the low level CD21 expression in these cultured epithelial cells in vitro reflects a biologically relevant process likely to constitute a feature of some epithelial cells in vivo.

CD21 RNA has been previously detected in the nasopharyngeal carcinoma cell lines C15 and C18 using a ribonuclease protection assay (46) providing an important precedent for these studies. However, the size or sequence of the CD21 RNAs in these cell lines was not determined, nor was protein expression examined. Further, these nasopharyngeal carcinoma cell lines are EBV infected. Previous studies have demonstrated that EBV can induce CD21 expression in B lymphocytes (46, 47).

A second important precedent was the demonstration of EBV receptors on epithelial cells by ultrastructural studies of virus binding to primary explant cultures of normal human uterine exocervix (48). Attempts to identify and characterize this receptor by immunological techniques, however, have led to conflicting results. Immunostaining studies using the HB-5a mAb have consistently demonstrated strong plasma membrane reactivity in epithelial cells of nasopharynx, tongue, tonsil, and uterine exocervix, as well as in some cultured epithelial cell lines (22–24, 26). Reactivity of tissues was generally described as confined to suprabasal spinous layers (18, 22, 23). Similar studies using the B2 antibody have revealed, in some cases, prominent membrane and cytoplasmic staining of epithelial cells (18, 22, 26). Other studies have failed to detect B2 reactivity (25), although the B2 epitope may have been sensitive to conditions of tissue fixation even if it had been present in sufficient abundance (26). Typically, all other CD21 antibodies, including OKB-7, failed to detect any epithelial cell antigens (24–26).

The seemingly conflicting results of these earlier studies may be accounted for in part by the data reported here. CD21 expression in RHEK-1 and HeLa cells was consistently low, and the glycoprotein was barely detectable with specific antibody or with the EBV ligand gp350/220. In RHEK-1 cells, which contained more CD21 mRNA than HeLa, demonstration of the 145-kD protein required high specific activity lysates from large numbers (10^8) of cells. Not surprisingly, repeated attempts to identify this protein in HeLa cells were unsuccessful because of substantially lower expression levels. In light of the low abundance of the CD21 protein in our studies, it is likely that the membrane staining observed using the HB-5a mAb is largely or entirely a consequence of detection of the previously described 195-kD protein. The ability of HB-5a to recognize this protein has been documented by us (Figs. 4, *A* and *B*; and 5, *A* and *C*) and others (22) through immunoprecipitation studies. Labeling by surface iodination confirms its association with the cell membrane. Nevertheless, this protein has no detectable gp350/220 binding activity and is unlikely to be an EBV receptor. It should be noted that HB-5a reactivity alone does not necessarily imply EBV binding properties since the EBV binding site and HB-5a epitope reside within physically separated CD21 SCRs (14–16).

CD21 is part of a multimolecular complex on the surface of B lymphocytes that includes CD19, TAPA-1, and Leu-13 (42, 43). In addition to biochemical evidence that CD19, CD21, TAPA-1, and Leu-13 form a multimolecular complex, cocapping and functional studies demonstrate that they normally associate on the cell surface (43). These observations are consistent with the possibility that CD19, CD21, TAPA-1, and Leu-13 assemble into a cell surface complex that may be involved in the generation of transmembrane signals related to receptor internalization. Since CD21 has the capacity to interact directly with the TAPA-1/Leu-13 complex, their presence on RHEK-1 cells is consistent with the possibility that CD21 and TAPA-1 may significantly associate on some epithelial cells.

These experiments also demonstrate that CD21 transcripts in both epithelial cells and B lymphocytes are initiated largely or predominantly from multiple sites located considerably upstream from previously identified initiation sites (12, 38). Observations in support of this conclusion include the identification of an epithelial cDNA clone initiating upstream of the previously mapped mRNA cap sites (Fig. 3, *A* and *B*); analysis by oligonucleotide hybridization and sequencing of 5′ RACE PCR amplification products generated from both epithelial and B lymphocyte cDNA (Fig. 3 *C*); and conventional PCR amplification of CD21 cDNA using oligonucleotide primers from the purported promoter region (data not shown). Heterogeneity among cloned IB4 PCR products and the diffuse nature of the PCR bands detected by hybridization suggest that multiple initiation sites may be utilized in CD21 gene transcription. Noteworthy in this regard is the lack of canonical CAAT and TATA box structures in the CD21 promoter. Absence of these structures is typically associated with heterogeneity in transcriptional initiation sites (49). An analogous situation exists in the promoter of the CD20 (B1) gene, which also lacks a canonical TATA box and initiates transcription from multiple sites (50). Initiation from upstream sites in the CD21 promoter may be related to GC-rich sequences, including AP-2 and SP1 elements present in this region (38). The sequence TATTT, located 30 nucleotides upstream of one previously mapped initiation site, has been proposed as a functional TATA box variant (38). A weak band detected by the CR-15 probe in amplified RHEK-1 cDNA (Fig. 3 *C*) may reflect low level utilization of the initiation site under the control of this element.

Initiation from an upstream site could affect CD21 polypeptide structure. The additional 5′ nucleotide sequence, which lacks a stop codon in frame with the CD21 reading frame, could potentially be translated to generate a novel protein distinguished from CD21 by additional amino terminal sequence. Absence of an in-frame initiator methionine codon anywhere in this region (38), however, makes this possibility unlikely.

Jong Rhim, Fred Wang, Alan Rickinson, and Lawrence Young contributed materials and advice.

This research was supported by grant CA-00449 from the National Cancer Institute (NCI) of the United States Public Health Service. M. Birkenbach is supported by Physicians Scientist Award K11CA01341 from NCI. T. F. Tedder is supported by grant AI-26872 from the National Institute of Allergy and Infectious Diseases, and is a scholar of the Leukemia Society of America.

Address correspondence to Mark Birkenbach, Department of Pathology, University of Chicago, 5841 S. Maryland Avenue, Chicago, IL 60637.

Received for publication 5 June 1992.

References

1. Henle, W., and G. Henle. 1985. Epstein-Barr virus and human malignancies. *Adv. Viral. Oncol.* 5:201.
2. Fingeroth, J.D., J.J. Weis, T.F. Tedder, J.L. Strominger, P.A. Biro, and D.T. Fearon. 1984. Epstein-Barr virus receptor of human B lymphocytes is the C3d receptor CR2. *Proc. Natl. Acad. Sci. USA.* 81:4510.
3. Nemerow, G.R., R. Wolfert, M.E. McNaughton, and N.R. Cooper. 1985. Identification and characterization of the Epstein-Barr virus receptor on human B lymphocytes and its relationship to the C3d complement receptor (CR2). *J. Virol.* 55:347.
4. Weis, J.J., T.F. Tedder, and D.T. Fearon. 1984. Identification of a 145,000 M_r membrane protein as the C3d receptor (CR2) of human B lymphocytes. *Proc. Natl. Acad. Sci. USA.* 81:881.
5. Tedder, T.F., L.T. Clement, and M.D. Cooper. 1984. Expression of C3d receptors during human B cell differentiation: immunofluorescence analysis with the HB-5 monoclonal antibody. *J. Immunol.* 133:678.
6. Tanner, J., J. Weis, D. Fearon, Y. Whang, and E. Kieff. 1987. Epstein-Barr virus gp350/220 binding to the B lymphocyte C3d receptor mediates adsorption, capping, and endocytosis. *Cell.* 50:203.

6a. Lozzio, C.B., and B.B. Lozzio. 1975. Human myelogenous leukemia cell-line with positive Philadelphia chromosome. *Blood.* 45:321.

7. Nemerow, G.R., R.A. Houghten, M.D. Moore, and N.R. Cooper. 1989. Identification of an epitope in the major envelope protein of Epstein-Barr virus that mediates viral binding to the B lymphocyte EBV receptor (CR2). *Cell.* 56:369.
8. Nemerow, G.R., and N.R. Cooper. 1984. Early events in the infection of human B lymphocytes by Epstein-Barr virus: the internalization process. *Virology.* 132:186.
9. Weis, J.J., and D.R. Fearon. 1985. The identification of N-linked oligosaccharides on the human CR2/Epstein-Barr virus receptor and their function in receptor metabolism, plasma membrane expression, and ligand binding. *J. Biol. Chem.* 260:13824.
10. Moore, M.D., N.R. Cooper, B.F. Tack, and G.R. Nemerow. 1987. Molecular cloning of the cDNA encoding the Epstein-Barr virus/C3d receptor (complement receptor type 2) of human B lymphocytes. *Proc. Natl. Acad. Sci. USA.* 84:9194.
11. Fujisaku, A., J.B. Harley, M.B. Frank, B.A. Gruner, B. Frazier, and V.M. Holers. 1989. Genomic organization and polymorphisms of the human C3d/Epstein-Barr virus receptor. *J. Biol. Chem.* 264:2118.
12. Weis, J.J., L.E. Toothaker, J.A. Smith, J.H. Weis, and D.T. Fearon. 1988. Structure of the human B lymphocyte receptor for C3d and the Epstein-Barr virus and relatedness to other members of the family of C3/C4 binding proteins. *J. Exp. Med.* 167:1047.
13. Moore, M.D., R.G. DiScipio, N.R. Cooper, and G.R. Nemerow. 1989. Hydrodynamic, electron microscopic, and ligand-binding analysis of the Epstein-Barr virus/C3dg receptor (CR2). *J. Biol. Chem.* 264:20576.
14. Martin, D.R., A. Yuryev, K.R. Kalli, D.T. Fearon, and J.M. Ahearn. 1991. Determination of the structural basis for selective binding of Epstein-Barr virus to human complement receptor type 2. *J. Exp. Med.* 174:1299.
15. Lowell, C.A., L.B. Klickstein, R.H. Carter, J.A. Mitchell, D.T. Fearon, and J.M. Ahearn. 1989. Mapping of the Epstein-Barr virus and C3dg binding sites to a common domain on complement receptor type 2. *J. Exp. Med.* 170:1931.
16. Carel, J.-C., B.L. Myones, B. Frazier, and V.M. Holers. Structural requirements for C3d,g/Epstein-Barr virus receptor (CR2/CD21) ligand binding, internalization, and viral infection. *J. Biol. Chem.* 265:12293.
17. Lemon, S.M., L.M. Hutt, J.E. Shaw, J.-L. Li, and J.S. Pagano. 1977. Replication for EBV in epithelial cells during infectious mononucleosis. *Nature (Lond.).* 268:268.
18. Talacko, A.A., C.G. Teo, B.E. Griffin, and N.W. Johnson. 1991. Epstein-Barr virus receptors but not viral DNA are present in normal and malignant oral epithelium. *J. Oral. Pathol. & Med.* 20:20.
19. zur Hausen, H., H. Schulte-Holthausen, G. Klein, W. Henle, G. Henle, P. Clifford, and L. Santesson. 1970. EB-virus DNA in biopsies of Burkitt tumors and anaplastic carcinomas of the nasopharynx. *Nature (Lond.).* 288:1056.
20. Löning, T., R.-P. Henke, P. Reichart, and J. Becker. 1987. In situ hybridization to detect Epstein-Barr virus DNA in oral tissues of HIV-infected patients. *Virchows Arch. A* 412:127.
21. Greenspan, J.S., D. Greenspan, E.T. Lennette, D.I. Abrams, M.A. Conant, V. Petersen, and U.K. Freese. 1985. Replication of Epstein-Barr virus within the epithelial cells of oral "hairy" leukoplakia, an AIDS-associated lesion. *N. Engl. J. Med.* 313:1564.
22. Young, L.S., C.W. Dawson, K.W. Brown, and A.B. Rickinson. 1989. Identification of a human epithelial cell surface protein sharing an epitope with the C3d/Epstein-Barr virus receptor molecule of B lymphocytes. *Int. J. Cancer.* 43:786.
23. Young, L.S., D. Clark, J.W. Sixbey, and A.B. Rickinson. 1986. Epstein-Barr virus receptors on human pharyngeal epithelia. *Lancet (N. Am. Ed.).* I:240.
24. Young, L.S., C.W. Dawson, and A.B. Rickinson. 1989. Epstein-

Barr virus/complement receptor and epithelial cells. *Lancet (N. Am. Ed.).* 2:448.
25. Niedobitek, G., H. Herbst, and H. Stein. 1989. Epstein-Barr virus/complement receptor and epithelial cells. *Lancet (N. Am. Ed.).* 2:110.
26. Timens, W., A. Boes, H. Vos, and S. Poppema. 1991. Tissue distribution of the C3d/EBV-receptor: CD21 monoclonal antibodies reactive with a variety of epithelial cells, medullary thymocytes, and peripheral T-cells. *Histochemistry.* 95:605.
27. Rhim, S.S., G. Jay, P. Arnstein, F.M. Price, K.K. Stanford, and S.A. Aaronson. 1985. Neoplastic transformation of human epidermal keratinocytes by AD12-SV40 and Kirsten sarcoma viruses. *Science (Wash. DC).* 227:1250.
28. Cooper, N.R., B.M. Bradt, J.S. Rhim, and G.R. Nemerow. 1990. CR2 complement receptor. *J. Invest. Dermatol.* 94:112S.
29. Jones, H.W., V.A. McKusick, P.S. Harper, and K.-D. Wuu. 1971. The HeLa cell and a reappraisal of its origin. *Obstet. Gynecol.* 38:945.
30. Bravo, R., J.V. Small, S.J. Fey, P.M. Larsen, and J.E. Celis. 1982. Architecture and polypeptide composition of HeLa cytoskeletons. *J. Mol. Biol.* 154:121.
31. Nadler, L.M., P. Stashenko, R. Hardy, A. van Agthoven, C. Terhorst, and S.F. Schlossman. 1981. Characterization of a human B cell specific antigen (B2) distinct from B1. *J. Immunol.* 126:1941.
32. Kansas, G.S., and T.F. Tedder. 1991. Transmembrane signals generated through MHC class II, CD19, CD20, CD39, and CD40 antigens induce LFA-1-dependent and independent adhesion in human B cells through a tyrosine kinase-dependent pathway. *J. Immunol.* 147:4094.
33. Oren, R., S. Takahashi, C. Doss, R. Levy, and S. Levy. 1990. TAPA-1, the target of an antiproliferative antibody, defines a new family of transmembrane proteins. *Mol. Cell. Biol.* 10:4007.
34. Chen, Y.X., K. Welte, D.H. Gebhard, and R.L. Evans. 1984. Induction of T cell aggregation by antibody to a 16 kd human leukocyte surface antigen. *J. Immunol.* 133:2496.
35. Chomczynski, P., and N. Sacchi. 1987. Single-step method of RNA isolation by acid guanidinium thiocyanate-phenol-chloroform extraction. *Anal. Biochem.* 162:156.
36. Li, Q.X., L.S. Young, G. Niedobitek, C.W. Dawson, M. Birkenbach, F. Wang, and A.B. Rickinson. 1992. Epstein-Barr virus infection and replication in a human epithelial cell system. *Nature (Lond.).* 356:347.
37. Frohman, M.A., M.K. Dush, and G.R. Martin. 1988. Rapid production of full-length cDNAs from rare transcripts: amplification using a single gene-specific oligo-nucleotide primer. *Proc. Natl. Acad. Sci. USA.* 85:8998.
38. Rayhel, E.J., M.H. Dehoff, and V.M. Holers. Characterization of the human complement receptor 2 (CR2, CD21) promoter reveals sequences shared with regulatory regions of other developmentally restricted B cell proteins. *J. Immunol.* 146:2021.
39. David, E.M., and A.J. Morgan. 1988. Efficient purification of Epstein-Barr virus membrane antigen gp340 by fast protein liquid chromatography. *J. Immunol. Methods.* 108:231.
40. Tanner, J., Whang, Y., Sample, J., Sears, A., and E. Kieff. 1988. Soluble gp350/220 and deletion mutant glycoproteins block Epstein-Barr virus adsorption to lymphocytes. *J. Virol.* 62:4452.
41. Toothaker, L.E., A.J. Henjes, and J.J. Weis. 1989. Variability of CR2 gene products is due to alternative exon usage and different CR2 alleles. *J. Immunol.* 142:3668.
42. Bradbury, L.E., G.S. Kansas, S. Levy, R.L. Evans, and T.F. Tedder. 1992. The CD19/CD21 signal transducing complex of human B lymphocytes includes the TAPA-1 and Leu-13 molecules. *J. Immunol.* In press.
43. Matsumoto, A.K., J. Kopicky-Burd, R.H. Carter, D.A. Tuveson, T.F. Tedder, and D.T. Fearon. 1991. Intersection of the complement and immune systems: a signal transduction complex of the B lymphocyte containing complement receptor type 2 and CD19. *J. Exp. Med.* 173:55.
44. Takahashi, S., C. Doss, S. Levy, and R. Levy. 1990. TAPA-1, the target of an antiproliferative antibody, is associated on the cell surface with the Leu-13 antigen. *J. Immunol.* 145:2207.
45. Ahearn, J.M., S.D. Hayward, J.C. Hickey, and D.T. Fearon. 1988. Epstein-Barr virus (EBV) infection of murine L cells expressing recombinant human EBV/C3d receptor. *Proc. Natl. Acad. Sci. USA.* 85:9307.
46. Billaud, M., P. Busson, D. Huang, N. Mueller-Lantzch, G. Rousselet, O. Pavlish, H. Wakasugi, J.M. Seigneurin, T. Tursz, and G.M. Lenoir. 1989. Epstein-Barr virus (EBV)-containing nasopharyngeal carcinoma cells express the B-cell activation antigen Blast2/CD23 and low levels of the EBV receptor CR2. *J. Virol.* 63:4121.
47. Wang, F., C. Gregory, C. Sample, R. Murray, D. Liebowitz, M. Rowe, A. Rickinson, and E. Kieff. 1990. Epstein-Barr virus latent infection membrane and nuclear proteins 2 and 3C are effectors of phenotypic changes in B lymphocytes: EBNA 2 and LMP cooperatively induce CD23. *J. Virol.* 64:2309.
48. Sixbey, J.W., D.D. Davis, L.S. Young, L. Hutt-Fletcher, T.F. Tedder, and A.B. Rickinson. 1987. Human epithelial cell expression of an Epstein-Barr virus receptor. *J. Gen. Virol.* 68:805.
49. Breathnach, R., and P. Chambon. 1981. Organization and expression of eucaryotic split genes coding for proteins. *Annu. Rev. Biochem.* 50:34.
50. Tedder, T.F., G. Klejman, S.F. Schlossman, and H. Saito. 1989. Structure of the gene encoding the human B lymphocyte differentiation antigen CD20 (B1). *J. Immunol.* 142:2560.